

ORIGINAL ARTICLE

MyD88-dependent signaling in non-parenchymal cells promotes liver carcinogenesis

Antje Mohs[†], Nadine Kuttkat[†], Tobias Otto[†], Sameh A. Youssef¹, Alain de Bruin^{1,2} and Christian Trautwein^{*}

Department of Internal Medicine III, University Hospital RWTH Aachen, Aachen Pauwelsstrasse 30, 52074, Germany,

¹Department of Pathobiology, Faculty of Veterinary Medicine, Dutch Molecular Pathology Center, Utrecht University, Yalelaan 1, 3508 TB Utrecht, The Netherlands and ²Department of Pediatrics, University Medical Center Groningen, University of Groningen, NL-9713 Groningen, The Netherlands

^{*}To whom correspondence should be addressed. Tel: +49 241 80 80866; Fax: +49 241 80 82455; Email: ctroutwein@ukaachen.de

[†]These authors contributed equally to this work.

Abstract

In Western countries, a rising incidence of obesity and type 2 diabetes correlates with an increase of non-alcoholic steatohepatitis (NASH)—a major risk factor for liver cirrhosis and hepatocellular carcinoma (HCC). NASH is associated with chronic liver injury, triggering hepatocyte death and enhanced translocation of intestinal bacteria, leading to persistent liver inflammation through activation of Toll-like receptors and their adapter protein myeloid differentiation factor 88 (MyD88). Therefore, we investigated the role of MyD88 during progression from NASH to HCC using a mouse model of chronic liver injury (hepatocyte-specific deletion of nuclear factor κ B essential modulator, Nemo; Nemo^{Δhepa}). Nemo^{Δhepa}, Nemo^{Δhepa}/MyD88^{-/-} and Nemo^{Δhepa}/MyD88^{Δhepa} were generated and the impact on liver disease progression was investigated. Ubiquitous MyD88 ablation (Nemo^{Δhepa}/MyD88^{-/-}) aggravated the degree of liver damage, accompanied by an overall decrease in inflammation, whereas infiltrating macrophages and natural killer cells were elevated. At a later stage, MyD88 deficiency impaired HCC formation. In contrast, hepatocyte-specific MyD88 deletion (Nemo^{Δhepa}/MyD88^{Δhepa}) did not affect disease progression. These results suggest that signaling of Toll-like receptors through MyD88 in non-parenchymal liver cells is required for carcinogenesis during chronic liver injury. Hence, blocking MyD88 signaling may offer a therapeutic option to prevent HCC formation in patients with NASH.

Introduction

Primary liver cancer is the sixth most common type of cancer and the second leading cause of cancer-related deaths worldwide with almost 800 000 deaths each year (1). Hepatocellular carcinoma (HCC) is the most common type of primary liver cancer and accounts for ~90% of the cases (2). In 90% of patients, HCC develops in a chronically injured and inflamed liver (2). The most frequent causes of chronic liver injury are viral infection such as hepatitis B and C, chronic alcohol abuse and non-alcoholic steatohepatitis (NASH) (2). With a rising incidence in Western countries, NASH represents an advanced stage of non-alcoholic fatty liver disease, in which metabolic alterations lead to chronic liver injury characterized by death of liver cells and subsequent inflammation (3).

During chronic liver injury, increased intestinal permeability causes translocation of bacterial products to the liver via the portal vein (4). These products are commonly termed pathogen-associated molecular patterns (PAMPs) and include lipopolysaccharide (LPS) and unmethylated CpG-containing DNA (4). Furthermore, chronic liver injury is characterized by increased occurrence of hepatocyte cell death leading to the release of various substances such as HMGB1 and mitochondrial DNA, which are collectively termed damage-associated molecular patterns (DAMPs) (5). Both PAMPs and DAMPs trigger activation of pattern recognition receptors of the Toll-like receptor (TLR) family (6). TLRs are transmembrane

Received: July 26, 2018; Revised: November 16, 2018; Accepted: January 31, 2019

© The Author(s) 2019. Published by Oxford University Press. All rights reserved. For Permissions, please email: journals.permissions@oup.com.

Abbreviations

CLD	chronic liver disease
DAMPS	damage-associated molecular patterns
DEN	N-nitrosodiethylamine
Ereg	epiregulin
HCC	hepatocellular carcinoma
HSC	hepatic stellate cell
IKK	inhibitor of NF- κ B kinase
IL	interleukin
LPS	lipopolysaccharide
MyD88	Myeloid differentiation factor 88
NASH	non-alcoholic steatohepatitis
NF- κ B	nuclear factor κ B
NK	natural killer
PAMPS	pathogen-associated molecular patterns
TLR	Toll-like receptor
TNF- α	tumor necrosis factor- α

receptors that are widely expressed on all liver cell types including immune cells (Kupffer cells and liver dendritic cells) as well as non-immune cells, e.g. hepatocytes, hepatic stellate cells (HSCs), sinusoidal endothelial cells and biliary epithelial cells (7). Myeloid differentiation factor 88 (MyD88) is a common adaptor protein for all TLRs (except TLR3) as well as for receptors of the interleukin (IL)-1 family (8). MyD88 primarily activates the transcription factor nuclear factor κ B (NF- κ B) resulting in the production of various pro-inflammatory cytokines including tumor necrosis factor α (TNF- α) and IL-6 (9). Consistent with this, MyD88 ablation in mice reduced the responsiveness of liver cells to PAMPS (e.g. LPS) and decreased liver inflammation and fibrosis after acute or chronic liver injury (10–13).

Tumor-promoting inflammation is regarded as one of the newly established enabling characteristics of cancer (14). Inflammation may promote cancer development through multiple mechanisms including inducing tissue remodeling, enhancing angiogenesis and providing growth factors. Therefore, TLRs and MyD88 not only link chronic liver injury to inflammation but could also promote carcinogenesis. Indeed, mice lacking MyD88 were shown to be resistant to intestinal adenoma formation in Apc^{Min/+} mice (15). In addition, MyD88^{-/-} mice exhibited reduced tumor formation in mouse models of carcinogen-induced HCC (16) and skin papillomas (17). During liver carcinogenesis, MyD88-dependent signaling was shown to be required for coupling hepatocyte cell death to a chronic inflammatory response mediated by Kupffer cells secreting tumor-promoting IL-6 (16). Consistent with the importance of MyD88 for TLR signaling, mice deficient for TLR4 also displayed a reduced development of carcinogen-induced HCC (18,19).

NF- κ B is a transcription factor, which can be activated in response to external inflammatory stimuli such as TNF- α , IL-1 and LPS (9). The intracellular transmission requires the action of the inhibitor of NF- κ B kinase [inhibitor of NF- κ B kinase (IKK)] complex, consisting of IKK α , IKK β and IKK γ (also known as Nemo) (9). Although Nemo does not contain kinase activity, it is essential for NF- κ B activation and mice constitutively lacking Nemo already die during embryogenesis because of massive TNF- α -induced apoptosis of hepatocytes (20). Hepatocyte-specific ablation of Nemo (termed Nemo^{Δhepa}) triggers hepatocyte apoptosis and chronic liver injury resembling human NASH (21). Importantly, these mice develop HCC by the age of 52 weeks (21). Therefore, they serve as a suitable experimental model for HCC development in a chronically injured liver.

To determine the importance of TLR signaling in liver cells during chronic liver disease (CLD), we investigated the impact of MyD88 deletion on disease progression in the Nemo^{Δhepa} model. Furthermore, we aimed to dissect whether this role of MyD88 signaling is specific to hepatocytes or non-parenchymal liver cells.

Materials and methods

Mouse generation and housing

To generate hepatocyte-specific knockout mice, we used a transgenic mouse strain (Alfp-Cre) expressing Cre recombinase under control of the albumin promoter regulatory elements and the α -fetoprotein enhancers, in combination with strains carrying floxed alleles of IKK γ /Nemo or MyD88 (22–24). Alfp-Cre-negative littermates (Nemo^{fl/fl}) served as controls. Hepatocyte-specific IKK γ /Nemo knockout mice (Nemo^{Δhepa}) mice were then crossed to either hepatocyte-specific MyD88 knockout mice (MyD88^{Δhepa}) or ubiquitously deleted MyD88 knockout mice (MyD88^{-/-}) to generate Nemo^{Δhepa}/MyD88^{Δhepa} or Nemo^{Δhepa}/MyD88^{-/-} mice (25). Animals were housed under specific pathogen-free conditions in the animal facility of the RWTH Aachen University. All animal experiments were carried out in line with the criteria of the Authority for Environment Conservation and Consumer Protection of the State of North Rhine-Westphalia (LANUV), Germany.

Blood analysis

Blood was collected from the vena cava inferior. In the blood serum, alanine transaminase, aspartate transaminase and alkaline phosphatase activity (ultraviolet test at 37°C) were measured at the Central Laboratory Facility of the University Hospital RWTH Aachen according to standard procedures. Whole blood was subjected to a complete blood count analysis at the Institute of Clinical Chemistry/Hematology of the RWTH Aachen University.

Histological staining and evaluation

Conventional hematoxylin and eosin staining was performed according to established protocols. The slides were evaluated microscopically by two board-certified veterinary pathologists (S.A.Y. and A.d.B.). Neoplastic lesions were classified as described previously (26). Non-neoplastic lesions were semi-quantitatively assessed for the following criteria: (i) hepatocellular anisokaryosis (polyploidy); (ii) foci of cellular alteration (altered foci); (iii) mitosis (non-neoplastic regions); (iv) apoptosis; (v) hepatocellular hypertrophy; (vi) lobular disorganization/dysplasia; (vii) oval cell hyperplasia; (viii) inflammation and (ix) other lesions. Scores were given as absent (0), subtle (1), mild (2), moderate (3), severe (4) and massive (5) with 0.5 interval for each criteria.

Cleaved caspase-3 staining was performed on formalin-fixed paraffin-embedded sections using a peroxidase-conjugated avidin-biotin method (Vectastain Elite ABC-HRP Kit; Vector Laboratories, Burlingame, CA). Sections were incubated with anti-cleaved caspase-3 antibody (1:1000, no. 9661; Cell Signaling). Visualization of the signal was performed using a 3,3'-diaminobenzidine substrate kit [DAB Peroxidase (HRP) Substrate Kit; Vector Laboratories]. Slides were counterstained with hematoxylin (Carl Roth, Karlsruhe, Germany).

Immunofluorescence staining was performed using liver cryosections. Cryosections were fixed using 4% formaldehyde and incubated with Ki-67 primary antibody (1:500, no. NCL-L-Ki67-MM1; Leica Biosystems, Wetzlar, Germany) overnight at 4°C. After washing, the sections were incubated with a fluorochrome-labeled secondary antibody (1:500; Thermo Fisher Scientific, Waltham, MA). Nuclei were counterstained using Vectashield Antifade Mounting Medium with 4',6'-diamidino-2-phenylindole (Vector Laboratories).

Imaging of histological sections was performed with an AxioImager Z1 (Carl Zeiss, Oberkochen, Germany) using AxioVision, version 4.2, software (Carl Zeiss).

Caspase-3 activity assay

Apoptosis was determined by quantification of specific caspase-3 enzyme activity (fluorescence units per microgram protein) in protein lysates from

whole-liver tissue, as described previously (27). In brief, protein lysates were incubated with the artificial substrate AFC-DEVD (Enzo Life Sciences, Lörrach, Germany) and the caspase-3-mediated release of AFC from DEVD was quantified by UV spectrometry.

Flow cytometry

First, capillary leukocytes were removed from the liver tissue by perfusion with phosphate-buffered saline. Then, the liver tissue was digested at 37°C using Collagenase II (Worthington, Lakewood, NJ). Afterwards, the liver was minced through a 70 µm cell strainer and remaining erythrocytes were lysed using BD Pharm Lyse buffer (BD Biosciences, San Jose, CA). The resulting cell suspension was stained with fluorochrome-conjugated antibodies (1:400) for myeloid cells (Mix 1) or lymphoid cells (Mix 2). Mix 1 contained Ly6G-FITC (no. 551460; BD Biosciences), Gr1.1-PerCP-Cy5.5 (no. 552093; BD Biosciences), CD11b-PE (no. 12-0112-83; Thermo Fisher Scientific), CD11c-APC (no. 17-0114-82; Thermo Fisher Scientific), F4/80-PE-Cy7 (no. 25-4801-82; Thermo Fisher Scientific), CD45-APC-eFluor780 (no. 47-0451-82; Thermo Fisher Scientific), Hoechst 33258 and BD Calibrite APC beads (no. 340487; BD Biosciences). Mix 2 contained CD8a-FITC (no. 11-0081-85; Thermo Fisher Scientific), CD4-PE (no. 12-0041-83; Thermo Fisher Scientific), NK1.1-PE-Cy7 (no. 25-5941-82; Thermo Fisher Scientific), CD3-APC (no. 12-0031-81; Thermo Fisher Scientific), CD45-APC-eFluor780 (no. 47-0451-82; Thermo Fisher Scientific), CD19-PerCP-Cy5.5 (no. 551001; BD Biosciences), Hoechst 33258 and BD Calibrite APC beads (BD Biosciences). Analysis was performed using a FACSCanto II system (BD Biosciences) and data were analyzed using FlowJo, version 7.5, software (FlowJo, Ashland, OR).

Cells were pre-gated on CD45 to identify leukocytes. Dead cells were excluded by Hoechst 33258. Neutrophil granulocytes were determined as Ly6G⁺ cells. Ly6G⁺ cells were further gated on CD11b^{high} and F4/80⁺ to determine monocyte-derived macrophages. Ly6G^{high} monocyte-derived macrophages were gated as Ly6G⁺ CD11b^{high} F4/80⁺ Gr1.1^{high}. Natural killer (NK) cells were identified as CD3⁺ NK 1.1⁺, T cells as CD3⁺ NK1.1⁺, natural killer T cells (NKT cells) as CD3⁺ NK1.1⁺, and B cells as CD19⁺ CD3⁺. Total cells per liver were calculated using BD Calibrite APC beads for calibration.

Tumor evaluation

Each liver was photographed with a Leica Z16 APO microscope (Leica Microsystems, Wetzlar, Germany) from every side. Tumors on the surface of each liver with at least 5 mm in diameter were evaluated. For each of these tumors, length and width were measured and the tumor size was calculated as size = length × width. For each mouse, the size of the largest tumor was plotted. In addition, cumulative tumor burden was calculated as sum of the size of all tumors in an individual mouse.

Reverse transcription-quantitative PCR analysis

Total RNA was isolated using peqGOLD RNAPure reagent (VWR International, Darmstadt, Germany). Reverse transcription was performed with random primers using the High-Capacity cDNA Reverse Transcription Kit (Thermo Fisher Scientific). Quantitative Real-Time PCR was performed using PowerUp SYBR Green reagent in a QuantStudio 5 Real-Time PCR System (Thermo Fisher Scientific). Relative mRNA expression was calculated using the $\Delta\Delta C_t$ method.

Statistical analysis

Data were analyzed using GraphPad Prism, version 5.0, software (GraphPad, La Jolla, CA) and are depicted as mean values with error bars indicating standard error of the mean. A one-way analysis of variance with Dunnett's multiple comparisons test was performed to compare each group with Nemo^{Ahepa} mice. Differences were considered significant when P values were below 0.05.

Results

In this study, we aimed to elucidate the role of MyD88 during CLD using a genetically engineered mouse model (Nemo^{Ahepa}), in which hepatocytes become selectively damaged. Thereby, this model allows monitoring the progression of CLD from early liver injury, inflammation and steatosis (resembling

NASH) to inflammation-induced HCC (21). We further aimed to differentiate between a role of MyD88 in these damaged hepatocytes and a function of MyD88 in non-parenchymal liver cells or immune cells. To this end, we generated mice with hepatocyte-specific deletion of MyD88 (MyD88^{Ahepa}) as well as mice with ubiquitous MyD88 ablation (MyD88^{-/-}). These mice were intercrossed with the NASH/HCC mouse model (Nemo^{Ahepa}). In all subsequent analyses, we focused on disease progression in male mice.

Ubiquitous deletion of MyD88 aggravates liver injury in Nemo^{Ahepa} mice

To analyze the early phase of CLD characterized by liver injury and inflammation, we assessed 8-week-old male mice. As expected, Nemo^{Ahepa} mice are characterized by high serum levels of liver transaminases, alanine transaminase and aspartate transaminase, indicating a high degree of liver injury resulting from hepatocyte cell death (Figure 1A and B). Furthermore, we observed strongly increased serum levels of liver transaminases in Nemo^{Ahepa} mice with concurrent ubiquitous MyD88 deletion, indicating elevated liver injury (Figure 1A). Although ubiquitous MyD88 deletion showed this profound impact on the degree of liver injury in Nemo^{Ahepa} mice, hepatocyte-specific MyD88 deletion did not alter the serum levels of liver transaminases (Figure 1B). Furthermore, we also detected increased serum levels of alkaline phosphatase, another (although less specific) marker for liver injury, in Nemo^{Ahepa} mice, and this was further elevated by ubiquitous (but not by hepatocyte-specific) MyD88 deletion (Figure 1C and D). In addition, we also determined serum levels of glutamate dehydrogenase, a mitochondrial enzyme that is released into the bloodstream specifically after hepatocyte cell death. In Nemo^{Ahepa} mice, glutamate dehydrogenase serum levels were strongly increased and although not statistically significant, additional ubiquitous (but not hepatocyte-specific) MyD88 deletion showed a trend toward higher glutamate dehydrogenase levels (Figure 1C and D). These results indicate that liver injury and hepatocyte cell death in Nemo^{Ahepa} mice are aggravated by ubiquitous ablation of MyD88 but unaltered by hepatocyte-specific MyD88 ablation.

These results were further corroborated by histopathological examination of liver tissues. Similar to the serum markers of liver injury, liver tissue sections showed profound liver damage (i.e. hepatocyte apoptosis, lobular dysplasia and inflammatory foci) in Nemo^{Ahepa} mice, which was aggravated in livers from mice with additional ubiquitous MyD88 deletion but unaltered after hepatocyte-specific MyD88 deletion (Figure 1E). Furthermore, the liver damage was multifocally randomly distributed (rather than periportal or pericentral) and this distribution was comparable between the different groups of mice.

Ubiquitous MyD88 ablation alters immune cell infiltration in response to liver injury

During chronic liver injury, translocation of intestinal microbial products (PAMPs) and release of intracellular substances (DAMPs) activate TLR signaling on a variety of cell types in the liver and contribute to induction of liver inflammation. As the majority of TLR signaling is dependent on the adapter protein MyD88, we expected that ablation of MyD88 might alter the inflammation-associated immune cell infiltration in the liver. Indeed, flow cytometry analysis revealed that infiltration with immune cells (identified by surface marker CD45) was induced in 8-week-old male Nemo^{Ahepa} mice and this was almost completely abolished by concurrent ubiquitous deletion

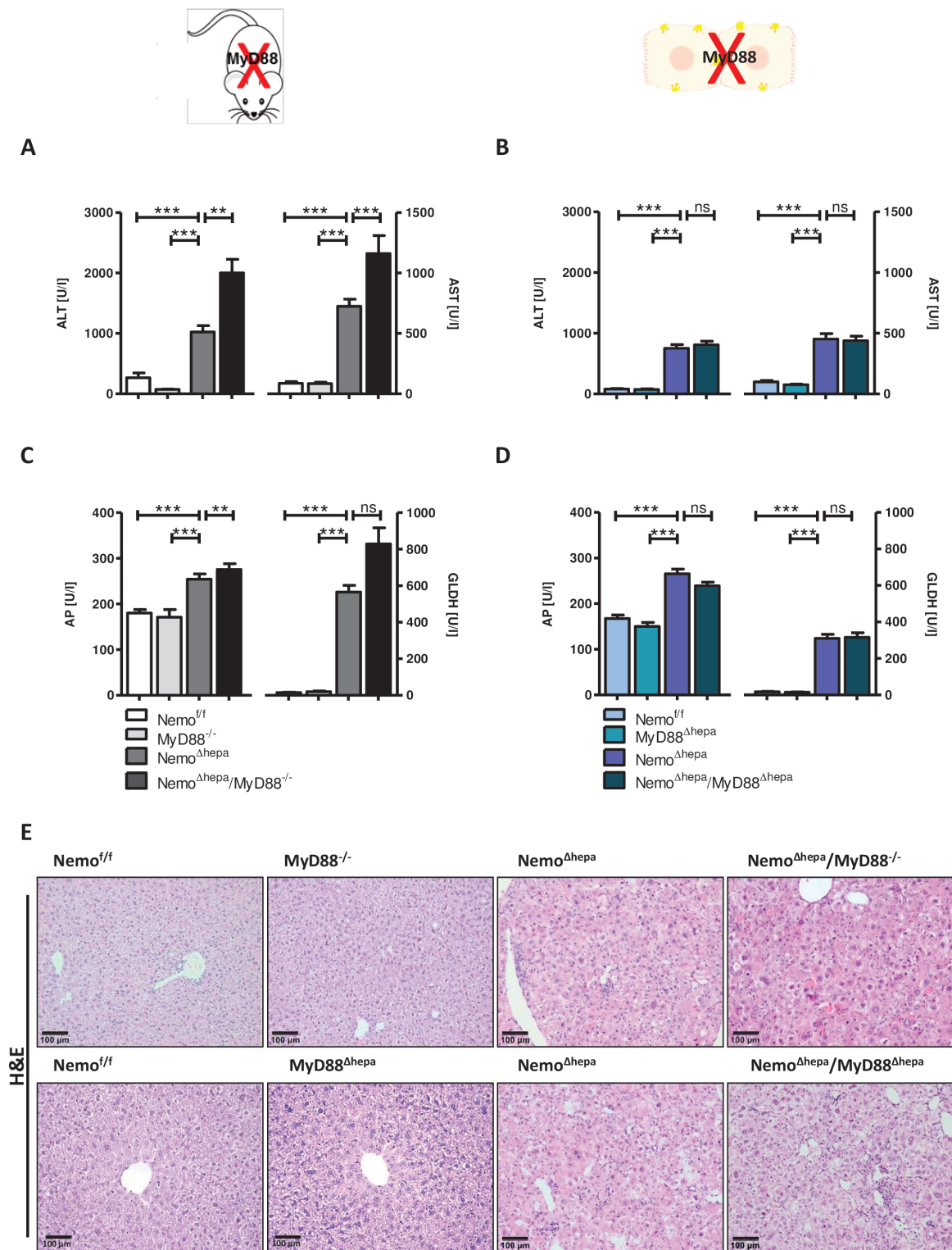


Figure 1. Ubiquitous MyD88 ablation enhances liver damage in male Nemo^{Δhepa} mice. (A, B) Serum levels of alanine transaminase (ALT) and aspartate transaminase (AST) in 8-week-old male Nemo^{fl/fl}, MyD88^{-/-}, Nemo^{Δhepa} and Nemo^{Δhepa}/MyD88^{-/-} mice (A), as well as in 8-week-old male Nemo^{fl/fl}, MyD88^{Δhepa}, Nemo^{Δhepa} and Nemo^{Δhepa}/MyD88^{Δhepa} mice (B). (C, D) Serum levels of alkaline phosphatase (AP) and glutamate dehydrogenase (GLDH) in 8-week-old male Nemo^{fl/fl}, MyD88^{-/-}, Nemo^{Δhepa} and Nemo^{Δhepa}/MyD88^{-/-} mice (C), as well as in 8-week-old male Nemo^{fl/fl}, MyD88^{Δhepa}, Nemo^{Δhepa} and Nemo^{Δhepa}/MyD88^{Δhepa} mice (D). (E) Histological sections of livers from 8-week-old male Nemo^{fl/fl}, MyD88^{-/-}, Nemo^{Δhepa} and Nemo^{Δhepa}/MyD88^{-/-} mice (upper panel), as well as from 8-week-old male Nemo^{fl/fl}, MyD88^{Δhepa}, Nemo^{Δhepa} and Nemo^{Δhepa}/MyD88^{Δhepa} mice (lower panel), stained with hematoxylin and eosin. Data represent mean ± SEM of at least eight mice per group; ***P < 0.001, **P < 0.01; ns, not significant; one-way analysis of variance (ANOVA) with Dunnett's multiple comparisons test comparing each group with Nemo^{Δhepa} mice; scale bars, 100 μm.

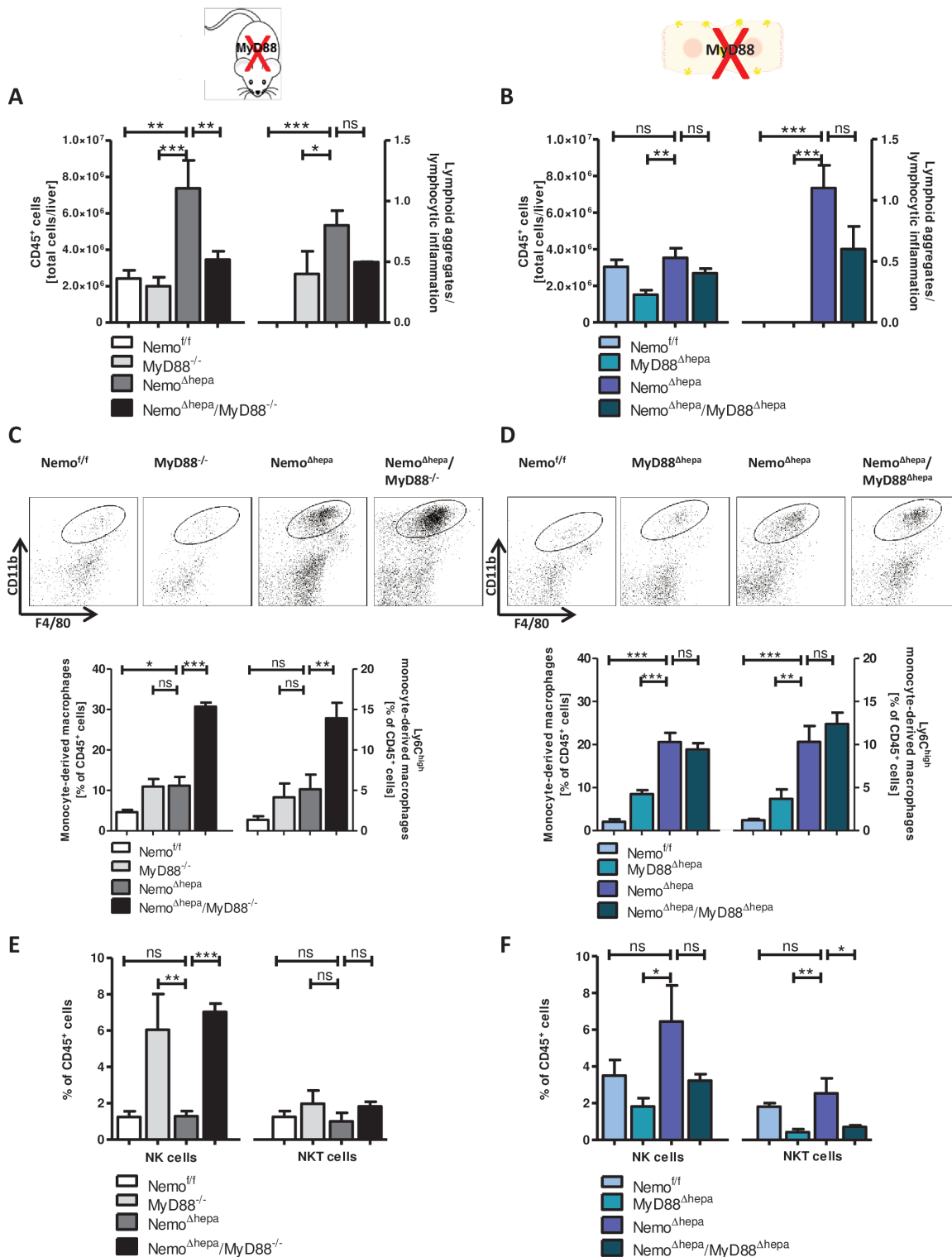


Figure 2. Ubiquitous MyD88 ablation affects immune cell infiltration in male *Nemo*^{Δhepa} mice. Flow cytometry and histopathological analysis of immune cells in livers from 8-week-old male *Nemo*^{+/f}, *MyD88*^{-/-}, *Nemo*^{Δhepa} and *Nemo*^{Δhepa}/*MyD88*^{-/-} mice (A, C, E), as well as from 8-week-old male *Nemo*^{+/f}, *MyD88*^{Δhepa}, *Nemo*^{Δhepa} and *Nemo*^{Δhepa}/*MyD88*^{Δhepa} mice (B, D, F). (A, B) Absolute numbers of CD45⁺ cells (leukocytes) per liver identified by flow cytometry (first four bars in each graph), as well as histopathological evaluation of the degree of lymphoid aggregates and lymphocytic inflammation (last four bars in each graph). (C, D) Flow cytometry analysis with representative dot plots of monocyte-derived macrophages identified by high F4/80 and high CD11b surface expression (top panels), as well as percentage of monocyte-derived macrophages (lower panel, first four bars in each graph) and Ly6C^{high} monocyte-derived macrophages (pro-inflammatory macrophages) (lower panel, last four bars in each graph) among CD45⁺ cells. (E, F) Percentage of NK cells (CD45⁺ NK1.1⁺ CD3⁻) (first four bars in each graph) and NKT cells (CD45⁺ NK1.1⁺ CD3⁺) (last four bars in each graph) among CD45⁺ cells identified by flow cytometry. Data represent mean ± SEM of at least four mice per group; ****P < 0.001, ***P < 0.01, **P < 0.05; ns, not significant; one-way analysis of variance (ANOVA) with Dunnett's multiple comparisons test comparing each group with *Nemo*^{Δhepa} mice.

of MyD88 (Figure 2A). In contrast, hepatocyte-specific MyD88 deletion did not alter immune cell infiltration (Figure 2B). Similar results were also obtained by histopathological evaluation of lymphoid aggregates and lymphocytic inflammation in liver sections of these mice (Figure 2A and B).

Macrophages represent the major cell type expressing TLRs and have been shown to be important mediators of liver inflammation and inflammatory cytokine production. Therefore, we quantified the percentage of monocyte-derived macrophages among infiltrating CD45⁺ cells in the liver using flow cytometry. Interestingly, Nemo^{hepa} mice with ubiquitous MyD88 deletion showed a strong increase in the percentage of infiltrating macrophages compared with Nemo^{hepa} mice (Figure 2C). This was not observed in Nemo^{hepa} mice with hepatocyte-specific MyD88 deletion (Figure 2D). Interestingly, the percentage of pro-inflammatory (Ly6C^{high}) macrophages was also markedly elevated in Nemo^{hepa} mice by ubiquitous (but not hepatocyte-specific) MyD88 deletion (Figure 2C and D).

We also analyzed infiltration of additional immune cell populations including T cells, CD4⁺ T helper cells, B cells and Ly6G⁺ cells (i.e. neutrophil granulocytes). For these immune cells, we did not observe significant alterations in livers of Nemo^{hepa} mice by concurrent ubiquitous (but not hepatocyte-specific) MyD88 deletion (Supplementary Figure 1A–D, available at Carcinogenesis Online). In contrast, we observed that the percentage of NK cells was increased in all mice with ubiquitous (but not hepatocyte-specific) MyD88 deletion (Figure 2E and F). We did not detect substantial changes in the infiltration of NKT cells (Figure 2E and F). These results indicate that, although overall immune cell infiltration in Nemo^{hepa} mice is severely impaired by the lack of the TLR adapter protein MyD88, pro-inflammatory monocyte-derived macrophages and NK cells are preferentially attracted into the livers.

Ubiquitous MyD88 deletion shows only a minor impact on apoptosis and proliferation following liver injury

As ubiquitous MyD88 ablation aggravated liver injury in the Nemo^{hepa} mouse model, we aimed to investigate whether this coincides with an increased portion of cells undergoing apoptosis, one of the major modes of hepatocyte cell death in a chronically injured liver. One of the best markers for apoptotic cell death is the activation of caspase-3. As expected, 8-week-old male mice with hepatocyte-specific Nemo deletion showed a strong increase in cells with cleaved caspase-3 and higher caspase-3 activity (Supplementary Figure 2A–D, available at Carcinogenesis Online). Mice with concurrent ubiquitous MyD88 deletion showed a trend toward a slightly higher number of cleaved caspase-3-positive cells as well as a higher caspase-3 activity in the liver, although this difference did not reach statistical significance (Supplementary Figure 2A and C, available at Carcinogenesis Online). Hepatocyte-specific MyD88 deletion did not affect the number of cleaved caspase-3-positive cells or the caspase-3 activity in Nemo^{hepa} livers (Supplementary Figure 2B and D, available at Carcinogenesis Online). Therefore, although we detected a potential slight increase in the extent of apoptotic cell death by ubiquitous deletion of MyD88 in Nemo^{hepa} mice, other modes of cell death may contribute to the elevated liver injury in these mice.

In response to hepatocyte cell death during liver injury, Kupffer cells can secrete IL-6 to stimulate compensatory proliferation of hepatocytes. This mechanism ensures liver regeneration and restoration of normal liver function. Thus, we were interested to assess the degree of compensatory

proliferation by liver injury resulting from hepatocyte-specific Nemo deletion in 8-week-old male mice. As expected, hepatocyte-specific Nemo deletion induced a strong induction of proliferation as indicated by the number of Ki-67⁺ cells and cells with mitotic nuclei (Supplementary Figure 3A–D, available at Carcinogenesis Online). Concurrent deletion of MyD88 (either ubiquitously or hepatocyte specific) displayed a slight trend toward lower proliferation (Supplementary Figure 3A–D, available at Carcinogenesis Online).

Ubiquitous MyD88 ablation reduces HCC development

After prolonged liver injury, mice with hepatocyte-specific deletion of Nemo develop inflammation-induced HCC at the age of 52 weeks (21). Tumor formation depends on the production of pro-inflammatory cytokines and growth factors triggered by TLR signaling. Because most TLR signaling is MyD88 dependent, we anticipated an impact of MyD88 ablation on HCC development.

Macroscopic liver examination revealed the presence of multiple solid tumors in 52-week-old male Nemo^{hepa} mice (Figure 3A and B). Importantly, the cumulative tumor burden, as well as the size of the largest tumor per mouse, was significantly reduced by concurrent ubiquitous (but not hepatocyte-specific) deletion of MyD88 (Figure 3A and B). Concomitantly, decreased tumor formation correlated well with reduced serum alanine transaminase levels and a reduced liver-to-body weight ratio in these double-mutant mice (Figure 3C and D). In contrast, we did not observe significant differences in overall tumor incidence or the incidence of different histological tumor type by MyD88 deletion in these mice (Supplementary Table 1, available at Carcinogenesis Online).

To further characterize the cellular changes associated with diminished HCC formation in Nemo^{hepa} livers by ubiquitous MyD88 deletion, we analyzed these tumors in more detail. Histopathological analysis revealed reduced tumor cell proliferation (as indicated by a reduced mitotic index) and reduced lymphoid aggregates and lymphocytic inflammation in the tumors of Nemo^{hepa} mice by ubiquitous MyD88 deletion (Figure 4A–C). Similarly, the number of circulating leukocytes was reduced in the peripheral blood of these mice (Figure 4D). This was further validated by flow cytometry analysis of immune cells in the livers. We detected a strong reduction in the number of CD45⁺ cells by concurrent ubiquitous MyD88 deletion in Nemo^{hepa} mice (Figure 4E). Similarly, the total number of infiltrating T cells was strongly diminished in these double mutant mice, whereas the percentage of T cells among CD45⁺ cells showed no significant difference (Figure 4F). To identify factors responsible for reduced tumor cell proliferation and lymphocytic infiltration, we analyzed normal liver tissue surrounding the tumors in these mice for expression changes of three previously described pro-tumorigenic factors, namely IL-6, TNF- α and epiregulin (Ereg) (16,18,19,28). Indeed, we demonstrated significantly reduced expression of IL-6 and TNF- α in Nemo^{hepa} livers by ubiquitous MyD88 deletion (Figure 4G).

These results indicate that MyD88-dependent TLR signaling in non-parenchymal liver cells plays an important role during progression from NASH to HCC, and blocking MyD88 function may be a potential therapeutic option to diminish inflammation-induced tumorigenesis in the liver.

Discussion

Chronic inflammation is an important promoter for carcinogenesis in the liver as well as in other organs. In ~90%

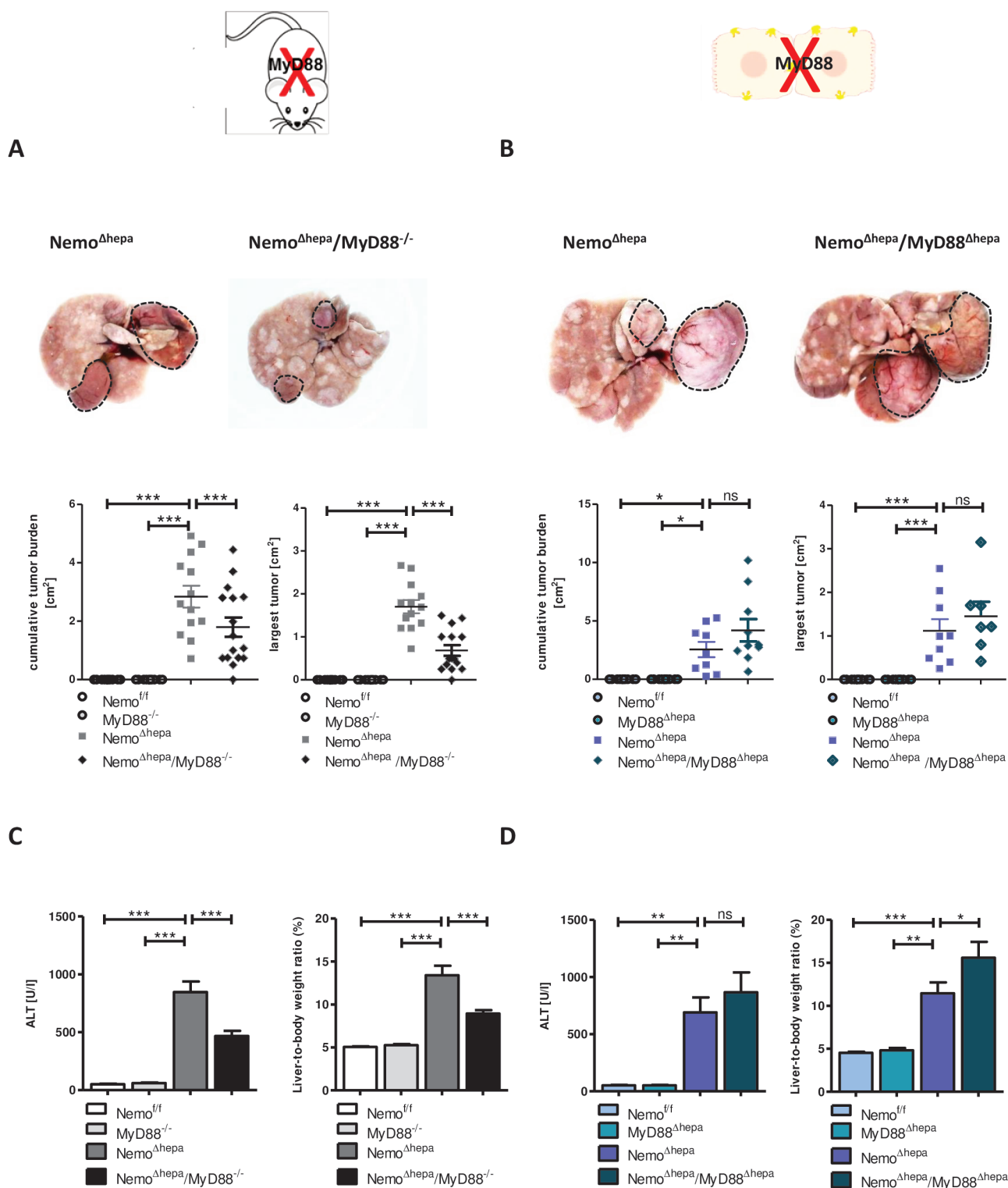


Figure 3. Ubiquitous MyD88 ablation reduces HCC development in male *Nemo*^{Δhepa} mice. (A, B) Macroscopic analysis of tumors in livers from 52-week-old male *Nemo*^{Δhepa}, *MyD88*^{-/-}, *Nemo*^{Δhepa} and *Nemo*^{Δhepa}/*MyD88*^{-/-} mice (A), as well as from 52-week-old male *Nemo*^{Δhepa}, *MyD88*^{Δhepa}, *Nemo*^{Δhepa} and *Nemo*^{Δhepa}/*MyD88*^{Δhepa} mice (B). Representative liver pictures are shown. Cumulative tumor burden and the size of the largest tumor per mouse were determined macroscopically. (C, D) Serum levels of ALT and liver-to-body weight ratio in 52-week-old male *Nemo*^{Δhepa}, *MyD88*^{-/-}, *Nemo*^{Δhepa} and *Nemo*^{Δhepa}/*MyD88*^{-/-} mice (C), as well as in 52-week-old male *Nemo*^{Δhepa}, *MyD88*^{Δhepa}, *Nemo*^{Δhepa} and *Nemo*^{Δhepa}/*MyD88*^{Δhepa} mice (D). Data represent mean ± SEM of at least four mice per group; ****P* < 0.001, ***P* < 0.01, **P* < 0.05; ns, not significant; one-way analysis of variance (ANOVA) with Dunnett's multiple comparisons test comparing each group with *Nemo*^{Δhepa} mice.

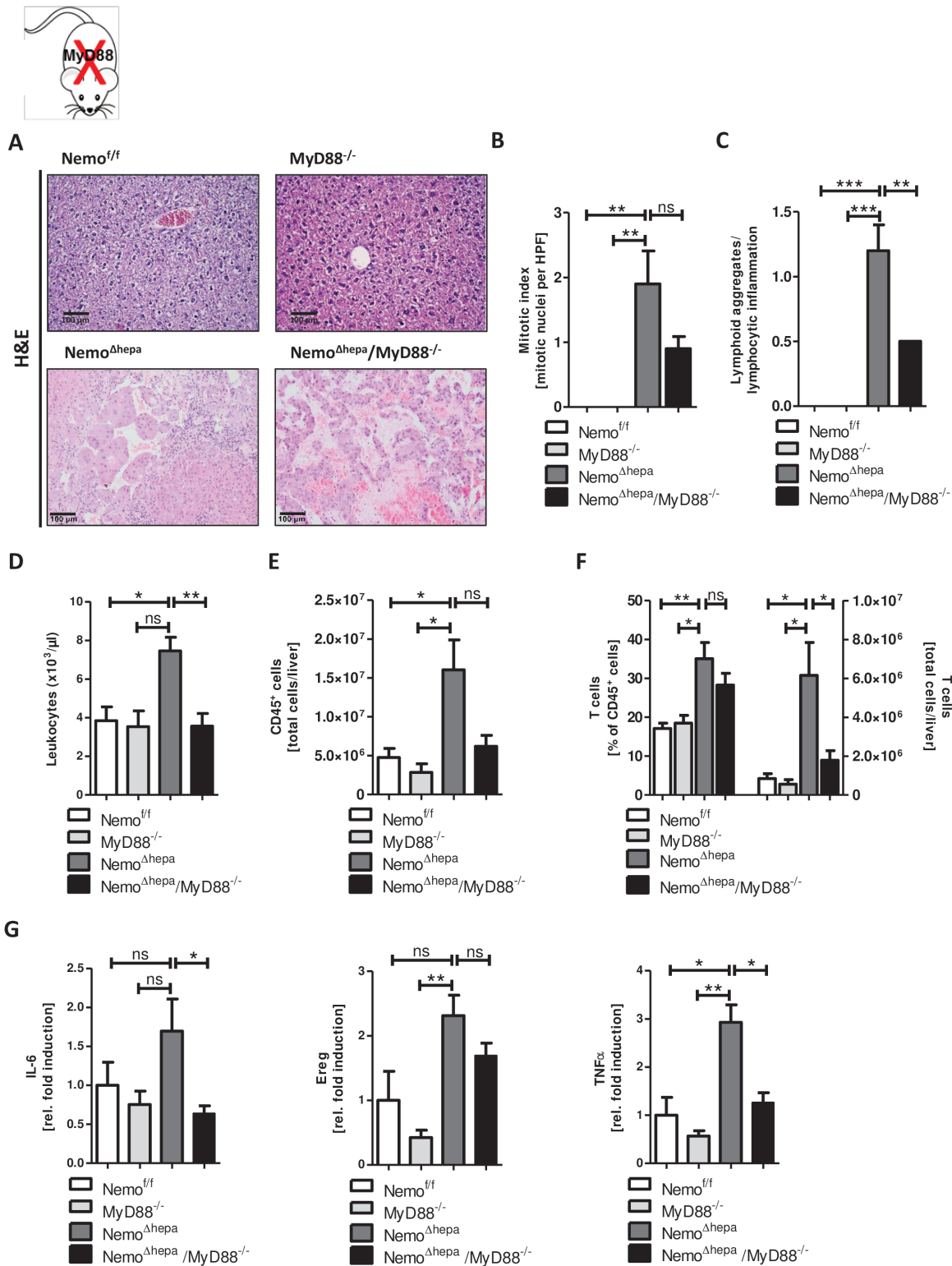


Figure 4. Ubiquitous MyD88 ablation reduces tumor cell proliferation and inflammation in male *Nemo^{Δhepa}* mice. (A) Histological sections of histologically normal livers from 52-week-old male *Nemo^{fl/fl}* and *MyD88^{-/-}* mice, and liver tumors (hepatocellular carcinomas) from 52-week-old male *Nemo^{Δhepa}* and *Nemo^{Δhepa}/MyD88^{-/-}* mice, stained with hematoxylin and eosin. (B) Quantification of the number of mitotic nuclei per high-power field (HPF) using histological sections depicted in (A). (C) Histopathological evaluation of the degree of lymphoid aggregates and lymphocytic inflammation using histological sections depicted in (A). (D) Number of leukocytes in peripheral blood from 52-week-old male *Nemo^{fl/fl}*, *MyD88^{-/-}*, *Nemo^{Δhepa}* and *Nemo^{Δhepa}/MyD88^{-/-}* mice. (E, F) Absolute numbers of CD45⁺ cells (E), T cells (F, last four bars) as well as the percentage of T cells among CD45⁺ cells (F, first four bars) identified by flow cytometry in livers from 52-week-old male *Nemo^{fl/fl}*, *MyD88^{-/-}*, *Nemo^{Δhepa}* and *Nemo^{Δhepa}/MyD88^{-/-}* mice. (G) RT-qPCR analysis of normal liver tissue from tumor-bearing 52-week-old male *Nemo^{fl/fl}*, *MyD88^{-/-}*, *Nemo^{Δhepa}* and *Nemo^{Δhepa}/MyD88^{-/-}* mice. Relative mRNA expression of IL-6, TNF- α , and Ereg was normalized to β -actin (Actb). Data represent mean \pm SEM of at least four mice per group; *** P < 0.001, ** P < 0.01, * P < 0.05; ns, not significant; one-way analysis of variance (ANOVA) with Dunnett's multiple comparisons test comparing each group with *Nemo^{Δhepa}* mice; scale bars, 100 μm .

of HCC cases, chronic inflammation precedes carcinogenesis and is associated with chronic liver injury (2). Furthermore, intestinal bacteria are also involved in inflammatory responses within the liver. Although the liver is not in direct contact with the microbiome of the gut, translocation of bacteria and bacterial products (PAMPS) may occur through the portal circulation and thereby contribute to liver inflammation. Moreover, this translocation is significantly enhanced during chronic liver injury because of elevated intestinal permeability (4). As a result, increased translocation of PAMPS and release of cellular products from dying liver cells (DAMPS) trigger activation of pattern recognition receptors during liver injury. These receptors are expressed on various liver cells including liver resident macrophages (i.e. Kupffer cells) and activate MyD88-dependent as well as MyD88-independent signaling pathways. In response, pro-inflammatory cytokines are released causing immune cell attraction and activation, thereby enhancing tumor promotion. Previous studies have suggested that deletion of MyD88 has a protective role during liver injury by reducing liver damage, inflammation, fibrosis and carcinogenesis (10–12,16,29). Therefore, we expected that ablation of MyD88 would ameliorate liver damage, inflammation and carcinogenesis in *Nemo^{Ahepa}* mice, an experimental model for chronic liver injury that displays progression to NASH and HCC (21).

As expected from these reports, we observed reduced immune cell infiltration in young *Nemo^{Ahepa}* mice by concurrent ubiquitous MyD88 deletion. Further analysis revealed that, although the overall immune cell infiltration in the liver was reduced, the percentage of NK cells and monocyte-derived macrophages, in particular pro-inflammatory (Ly6C^{high}) macrophages, was significantly elevated by MyD88 deletion. Surprisingly, we also observed an increase in liver damage. In these mice, ablation of IKK γ (*Nemo*) abrogates NF- κ B signaling specifically in hepatocytes. Although NF- κ B orchestrates numerous functions during inflammation, it also induces proliferation and survival in several cell types (9). For instance, it protects hepatocytes from oxidative stress-dependent apoptotic cell death (21). Furthermore, inhibition of NF- κ B signaling by deletion of its activator *Nemo* leads to increased levels of the death receptor DR5 on the cell surface of hepatocytes, thereby making them hypersensitive to apoptosis induced by TNF-related apoptosis-inducing ligand, a ligand for DR5 (24). Notably, NK cells, the main source of TNF-related apoptosis-inducing ligand (TRAIL), were activated in *Nemo^{Ahepa}* mice and depletion of NK1.1⁺ cells (i.e. NK and NKT cells) reduced liver damage in these mice (24). Therefore, elevated infiltration of NK cells in the livers of MyD88-deficient *Nemo^{Ahepa}* mice may elicit increased cell death of hepatocytes and, hence, contribute to aggravated liver damage in these mice.

Interestingly, mice with MyD88 deficiency are well known for being particularly susceptible to pathogenic infections by bacteria, viruses and fungi (30). This also mirrors the increased incidence of life-threatening infections in humans with hereditary MyD88 deficiency (30). Mechanistically, mice lacking MyD88 displayed delayed clearance of bacterial infections because of reduced recruitment of CD4⁺ T cells, as well as an incapability of NK cells to produce interferon γ (31). This defect was also associated with locally decreased levels of the NK cell activators IL-17, IL-18 and TNF- α , as well as increased levels of the chemokine CCL2 triggering increased macrophage recruitment as a potential compensatory mechanism (31). Indeed, we also observed reduced recruitment of CD4⁺ T cells and increased macrophage recruitment to the livers of

MyD88-deficient *Nemo^{Ahepa}* mice. It is therefore conceivable that *Nemo^{Ahepa}* mice with MyD88 deficiency display partially impaired bacterial clearance and increased bacterial burden in the liver, which is possibly associated with the observed increase in monocyte-derived macrophages. Although the levels of infiltrating monocyte-derived macrophages are only slightly elevated in MyD88-deficient *Nemo^{Ahepa}* mice, they may also contribute to aggravated liver damage in these mice. Indeed, a previous study showed that depletion of Kupffer cells using clodronate-loaded liposomes prevents infiltration of pro-inflammatory (Ly-6C^{high}) macrophages and protects from liver damage and steatohepatitis in a mouse model of NASH (32). Moreover, another report demonstrated that specific inhibition of macrophage infiltration using a pharmacological inhibitor of the macrophage-attracting chemokine CCL2 diminishes liver steatosis in a mouse model of NASH (33). Therefore, we speculate that a potentially increased bacterial burden and elevated macrophage infiltration may contribute to enhanced liver damage observed in MyD88-deficient *Nemo^{Ahepa}* mice.

Previous studies suggested that intestinal microbiota and signaling through MyD88-dependent receptors such as TLRs is crucial for generating an inflammatory environment in a chronically injured liver that facilitates cancer formation. For instance, mice lacking TLR4 were partially resistant to tumorigenesis induced either by *N*-nitrosodiethylamine (DEN), a carcinogen, or by a combination of DEN and repeated carbon tetrachloride administration (18,19). At the same time, HCC formation was augmented by intestinal bacteria and could be diminished by antibiotic treatment (18,19). This tumor-promoting effect of TLR4 signaling was mediated by liver resident cells such as Kupffer cells or HSCs, and not by bone-marrow-derived immune cells (18). Interestingly, antibiotic treatment reduced the production of IL-6 and TNF- α in DEN-treated mice, two cytokines that were previously shown to be produced by Kupffer cells and to enhance hepatocyte growth (19,28). Although one study demonstrated that bacterial products (e.g. LPS) can also promote HSC-dependent production of the mitogen *Ereg*, ablation of *Ereg* expression in mice treated with DEN and carbon tetrachloride only modestly reduced HCC formation (18). Therefore, *Ereg* might not be the main driver for liver carcinogenesis. Although TLR4 can signal through MyD88 as well as through TRIF, TLR9 signaling exclusively depends on MyD88 as an adapter protein (8). Similar to the role of TLR4, TLR9-deficient mice displayed a reduced susceptibility to liver carcinogenesis (29). In contrast, another group reported that in the absence of chronic liver injury, deficiency in either TLR4 or TLR2 enhanced carcinogen-induced HCC formation in mice (34,35). Although these studies indicate differences in the role of TLR signaling depending on the degree of liver injury and inflammation, they suggest a tumor-promoting role of MyD88-dependent receptors in a chronically injured liver.

In this study, we investigated the role of MyD88-dependent signaling in a genetically engineered mouse model (*Nemo^{Ahepa}*), in which hepatocytes become selectively damaged, triggering chronic liver injury and disease progression to HCC (21). In line with a study investigating carcinogen-induced HCC (16), we observed decreased HCC formation in 52-week old male *Nemo^{Ahepa}* mice ubiquitously lacking MyD88. This was accompanied by reduced liver damage and diminished liver inflammation. We also noticed a trend toward decreased proliferation within the tumors of MyD88-deficient mice. Earlier studies suggested that TLR/MyD88 signaling contributes to tumor promotion by

enhancing the production of mitogens, e.g. IL-6 and TNF- α by Kupffer cells, as well as Ereg by HSCs (16,18,19). Notably, we observed significantly reduced expression of IL-6 and TNF- α , but not Ereg, in MyD88-deficient Nemo^{Ahepa} mice. This suggests that Kupffer cells are the major cell type involved in MyD88-dependent HCC promotion in Nemo^{Ahepa} mice. Nevertheless, it remains possible that MyD88-dependent signaling in HSCs also contributes to tumor formation in these mice. Interestingly, increased serum levels of estrogens in female mice not only diminished MyD88-dependent production of IL-6 by Kupffer cells but also severely impaired liver carcinogenesis in DEN-treated mice (16). Furthermore, in a previous study, we showed that complete blocking of IL-6 signaling in hepatocytes by gp130 deletion attenuated HCC formation in DEN-treated mice (36). This confirms IL-6, produced mainly by Kupffer cells, as major cytokine mediating the tumor-promoting effects of MyD88 signaling.

Although we observed substantial and significant changes in liver damage and tumor formation by ubiquitous deletion of MyD88 in Nemo^{Ahepa} mice, hepatocyte-specific deletion of MyD88 showed only insignificant or negligible effects. This would suggest that signaling through MyD88-dependent pattern recognition receptors is only essential in non-parenchymal liver cells (e.g. Kupffer cells or HSCs) during disease progression in chronic liver injury and liver carcinogenesis. However, previous studies showed that hepatocytes express MyD88 (as well as a variety of TLRs) and are dependent on MyD88 signaling for their response to bacterial products such as LPS (37–39). Of note, the majority of cellular effects of MyD88-dependent receptor signaling are mediated by the transcription factor NF- κ B (9). In Nemo^{Ahepa} mice, hepatocytes lack IKK γ (Nemo), an essential component of the NK- κ B-activating IKK complex, and are hence unable to signal through the NF- κ B pathway (9). Therefore, in our mouse model, we are unable to determine whether signaling through the NF- κ B-dependent MyD88 signaling in hepatocytes may contribute to disease progression. Despite this limitation, our results show that NF- κ B-independent signaling in hepatocytes is not essential during chronic liver injury and liver carcinogenesis.

In conclusion, we show that deficiency in MyD88-dependent receptor signaling within non-parenchymal liver cells modulates tumor-promoting inflammation associated with chronic liver injury. Although this enhances liver damage in early stages, liver carcinogenesis is diminished in late stages of chronic liver injury. As suggested by other studies, this tumor-promoting effect is most probably mediated by Kupffer cell-dependent production of inflammatory cytokines and mitogenic factors, most importantly IL-6.

Supplementary material

Supplementary data are available at Carcinogenesis online.

Funding

Deutsche Forschungsgemeinschaft to C.T. (TR285/10–1); Faculty of Medicine at the RWTH Aachen University (IZKF Oncology P06 to T.O. and C.T.).

Acknowledgements

We thank Shizuo Akira for providing MyD88^{-/-} mice.

Conflict of Interest Statement: None declared.

References

1. Ferlay, J. et al. (2015) Cancer incidence and mortality worldwide: sources, methods and major patterns in GLOBOCAN 2012. *Int. J. Cancer*, 136, E359–E386.
2. Llovet, J.M. et al. (2016) Hepatocellular carcinoma. *Nat. Rev. Dis. Primers*, 2, 16018.
3. Ringelhan, M. et al. (2018) The immunology of hepatocellular carcinoma. *Nat. Immunol.*, 19, 222–232.
4. Seki, E. et al. (2012) Role of innate immunity and the microbiota in liver fibrosis: crosstalk between the liver and gut. *J. Physiol.*, 590, 447–458.
5. Kubes, P. et al. (2012) Sterile inflammation in the liver. *Gastroenterology*, 143, 1158–1172.
6. Salcedo, R. et al. (2013) MyD88 and its divergent toll in carcinogenesis. *Trends Immunol.*, 34, 379–389.
7. Roh, Y.S. et al. (2013) Toll-like receptors in alcoholic liver disease, non-alcoholic steatohepatitis and carcinogenesis. *J. Gastroenterol. Hepatol.*, 28 (suppl. 1), 38–42.
8. Yamamoto, M. et al. (2010) Current views of toll-like receptor signaling pathways. *Gastroenterol. Res. Pract.*, 2010, 240365.
9. Taniguchi, K. et al. (2018) NF- κ B, inflammation, immunity and cancer: coming of age. *Nat. Rev. Immunol.*, 18, 309–324.
10. Seki, E. et al. (2007) TLR4 enhances TGF- β signaling and hepatic fibrosis. *Nat. Med.*, 13, 1324–1332.
11. Miura, K. et al. (2010) Toll-like receptor 9 promotes steatohepatitis by induction of interleukin-1 β in mice. *Gastroenterology*, 139, 323–34. e7.
12. Ojito, K. et al. (2010) MyD88-dependent pathway accelerates the liver damage of Concanavalin A-induced hepatitis. *Biochem. Biophys. Res. Commun.*, 399, 744–749.
13. Kawai, T. et al. (1999) Unresponsiveness of MyD88-deficient mice to endotoxin. *Immunity*, 11, 115–122.
14. Hanahan, D. et al. (2011) Hallmarks of cancer: the next generation. *Cell*, 144, 646–674.
15. Rakoff-Nahoum, S. et al. (2007) Regulation of spontaneous intestinal tumorigenesis through the adaptor protein MyD88. *Science*, 317, 124–127.
16. Naugler, W.E. et al. (2007) Gender disparity in liver cancer due to sex differences in MyD88-dependent IL-6 production. *Science*, 317, 121–124.
17. Swann, J.B. et al. (2008) Demonstration of inflammation-induced cancer and cancer immunoediting during primary tumorigenesis. *Proc. Natl. Acad. Sci. U. S. A.*, 105, 652–656.
18. Dapito, D.H. et al. (2012) Promotion of hepatocellular carcinoma by the intestinal microbiota and TLR4. *Cancer Cell*, 21, 504–516.
19. Yu, L.X. et al. (2010) Endotoxin accumulation prevents carcinogen-induced apoptosis and promotes liver tumorigenesis in rodents. *Hepatology*, 52, 1322–1333.
20. Rudolph, D. et al. (2000) Severe liver degeneration and lack of NF- κ B activation in NEMO/IKK γ -deficient mice. *Genes Dev.*, 14, 854–862.
21. Luedde, T. et al. (2007) Deletion of NEMO/IKK γ in liver parenchymal cells causes steatohepatitis and hepatocellular carcinoma. *Cancer Cell*, 11, 119–132.
22. Hou, B. et al. (2008) Toll-like receptors activate innate and adaptive immunity by using dendritic cell-intrinsic and -extrinsic mechanisms. *Immunity*, 29, 272–282.
23. Kellendonk, C. et al. (2000) Hepatocyte-specific expression of Cre recombinase. *Genesis*, 26, 151–153.
24. Beraza, N. et al. (2009) Hepatocyte-specific NEMO deletion promotes NK/NKT cell- and TRAIL-dependent liver damage. *J. Exp. Med.*, 206, 1727–1737.
25. Adachi, O. et al. (1998) Targeted disruption of the MyD88 gene results in loss of IL-1- and IL-18-mediated function. *Immunity*, 9, 143–150.
26. Thoolen, B. et al. (2010) Proliferative and nonproliferative lesions of the rat and mouse hepatobiliary system. *Toxicol. Pathol.*, 38(suppl. 7), 5S–81S.
27. Liedtke, C. et al. (2007) Molecular mechanism of Mitomycin C-dependent caspase-8 regulation: implications for apoptosis and synergism with interferon- α signalling. *Apoptosis*, 12, 2259–2270.

28. Maeda, S. et al. (2005) IKKbeta couples hepatocyte death to cytokine-driven compensatory proliferation that promotes chemical hepatocarcinogenesis. *Cell*, 121, 977–990.
29. Song, I.J. et al. (2018) The contribution of toll-like receptor signaling to the development of liver fibrosis and cancer in hepatocyte-specific TAK1-deleted mice. *Int. J. Cancer*, 142, 81–91.
30. von Bernuth, H. et al. (2012) Experimental and natural infections in MyD88- and IRAK-4-deficient mice and humans. *Eur. J. Immunol.*, 42, 3126–3135.
31. Nagarajan, U.M. et al. (2011) MyD88 deficiency leads to decreased NK cell gamma interferon production and T cell recruitment during *Chlamydia muridarum* genital tract infection, but a predominant Th1 response and enhanced monocytic inflammation are associated with infection resolution. *Infect. Immun.*, 79, 486–498.
32. Reid, D.T. et al. (2016) Kupffer cells undergo fundamental changes during the development of experimental NASH and are critical in initiating liver damage and inflammation. *PLoS One*, 11, e0159524.
33. Baeck, C. et al. (2012) Pharmacological inhibition of the chemokine CCL2 (MCP-1) diminishes liver macrophage infiltration and steatohepatitis in chronic hepatic injury. *Gut*, 61, 416–426.
34. Lin, H. et al. (2013) Antioxidant N-acetylcysteine attenuates hepatocarcinogenesis by inhibiting ROS/ER stress in TLR2 deficient mouse. *PLoS One*, 8, e74130.
35. Wang, Z. et al. (2013) Toll-like receptor 4 activity protects against hepatocellular tumorigenesis and progression by regulating expression of DNA repair protein Ku70 in mice. *Hepatology*, 57, 1869–1881.
36. Hatting, M. et al. (2015) Lack of gp130 expression in hepatocytes attenuates tumor progression in the DEN model. *Cell Death Dis.*, 6, e1667.
37. Lee, Y.S. et al. (2017) Hepatocyte toll-like receptor 4 mediates lipopolysaccharide-induced hepcidin expression. *Exp. Mol. Med.*, 49, e408.
38. Chen, C. et al. (2014) Lipopolysaccharide stimulates p62-dependent autophagy-like aggregate clearance in hepatocytes. *Biomed Res. Int.*, 2014, 267350.
39. Liu, S. et al. (2002) Role of toll-like receptors in changes in gene expression and NF-kappa B activation in mouse hepatocytes stimulated with lipopolysaccharide. *Infect. Immun.*, 70, 3433–3442.